Optical Properties of Gold Atoms in γ-Irradiated Organic Solid Solutions at 77 K

Yoko Miyatake Hase*

Department of Mechanical Science and Bioengineering, Graduate School of Engineering Science, Osaka University, Toyonaka, Osaka, 560-8531 Japan

Takeshi Saito†

Research Reactor Institute, Kyoto University, Kumatori-cho, Osaka, 590-0494 Japan

Yusuke Tajima‡ **and Mikio Hoshino**§

The Institute of Physical and Chemical Research, Wako-si, Saitama, 351-0198 Japan

Received: June 6, 2003; In Final Form: December 8, 2003

Au^0 atoms were produced via the electron capture of Au^+ ions in γ-irradiated solid solutions of MTHF at 77 K. The optical absorption bands observed in the regions of UV and NUV are ascribed to Au^0. The steady-state emission and excitation spectra were measured by photoexcitation at 73 K before and after γ-irradiation of the solid solutions containing [Au^+] ions. The two-dimensional time-resolved emission spectra were also investigated by photoexcitation at $\lambda_{exc} = 337$, 380, and 420 nm by using an N_2 laser and dye lasers. A set of five emission bands of 385, 430, 480, 520, and 580 nm and another set of emission bands at 456, 482, 484, and 520 nm were observed. The latter set of emission bands showed such characteristic structures as the mirror image of the absorption bands of Au^0 in the rare gas matrixes. The emission band at 430 nm observed before γ-irradiation was confirmed to be phosphorescence due to Au^+ with a lifetime of about 625 ms. A part of the emission band of 385 nm observed after γ-irradiation was also due to phosphorescence consisting of two components with lifetimes of 146 and 461 ms. Three types of exciplexes (Au^+·L*n*)*, (Au^0·L*n*...Au^+)*, (Au^0·L*n*)*, and the excited gold atom (Au^0)* are proposed for all the emission bands including phosphorescence. The excited gold atoms in $2P_{1/2}$ and $2P_{3/2}$ states participate mainly in the formation of these emissive exciplexes. The formation mechanism for these species is also presented.

Introduction

Magnetic and optical properties of 1B metal atoms produced radiation-chemically by reducing their mono cations in condensed matter have been investigated[1−7] as a fundamental research to elucidate the function and effects of metal ions and/or atoms in biological systems.

1B metal atoms have long been the targets of various research studies because of their simple electronic structures. Especially, the atoms in the gas phase at low temperatures are isolated from electrostatic fields of neighboring ions, atoms, or gas molecules, so that their energy levels and various physicochemical properties have been well established and systematically published.[8] Several important studies on interaction between the isolated 1B metal atoms prepared by co-condensation method in rare gas matrixes have also been reported.[9−15] On the other hand, except for the case of silver atoms at low temperatures as reported previously,[1−5] few studies have been carried out for other 1B metal atoms to elucidate the solute−solute or solute−solvent interactions which are induced by the atoms or ions surrounded by water or organic molecules. Many problems involving the optical properties of the atoms or ions in these environments remain unsolved, especially for the case of the gold atom. There have been a limited number of emission or fluorescence studies on gold atoms in condensed matter, though interest in this has increased recently from the viewpoint of nanoparticle science.[16,17] The present study is expected to give an effective suggestion for solving the remaining problems in condensed matter by comparing to well-established information in gas phase and in solid rare gas matrixes.

To distribute metal atoms with a spatial uniformity in matrixes, we have used radiation chemical reduction of aqueous or organic solutions containing monovalent metal ions at low temperatures.[1−7]

In previous studies, silver (Ag^0)[1−5] and copper (Cu^0)[7] atoms were produced via electron capture by the metal ions in γ-irradiated organic solid solutions at 77 K, and the ESR, optical absorption, and emission characteristics were investigated. Evidence for the formation of the dimer cation was confirmed by ESR observation in the case of Ag^0 but not for Cu^0. The photoionization of the metal atoms in their excited states, (Ag^0)* and (Cu^0)*, occurred by photoexcitation in the wavelength region of 350−450 nm and around 250 nm of the absorption bands, respectively. The emission and excitation spectra revealed that the metal atoms in their excited states coupled with solvent molecules and formed characteristic emissive exciplexes.

The first ESR report of gold atoms (Au^0) which were produced radiation-chemically by reducing Au^+ ions was presented in our previous study.[6] We used the two sets of solute−solvent combination of $AuClP(C_2H_5)_3$ in 2-methyltetra-

* Author to whom all correspondence should be addressed. E-mail: miyatake@me.es.osaka-u.ac.jp.
† E-mail: ta-saito@HL.rri.kyoto-u.ac.jp.
‡ E-mail: tajima@postman.riken.go.jp.
§ E-mail: hoshino@postman.riken.go.jp.

10.1021/jp035599e CCC: $27.50
Published on Web 01/29/2004

hydrofuran (MTHF) and AuCN in 10 M NaOH. We have confirmed Au^0 atoms in the solid solutions by observing the characteristic ESR absorption lines of Au^0. The hyperfine coupling constant, a, and the g-value were calculated by using Breit-Rabi equations. The relative shift of the values of a, i.e., $(a - a_{free})/a_{free}$ was -16%, indicating that delocalization of the spin density of Au^0 onto ligands occurs as well as for Ag^0 (-13%), but less than in the case of Cu^0 (-50%). The relative shift of the g-values, i.e., $(g_J - g_{Jfree})$ was positive which is similar to the case of Cu^0, though a negative shift was obtained for Ag^0. The possible explanation is proposed that the admixture of the wave function of the atom in its ground state, i.e., $2S_{1/2}$ into d orbital is expected to occur to some extent for the Au^0 and Cu^0, rather than p orbital which is expected to occur for Ag^0.

To elucidate the absorption and emission mechanism of Au^0, we have further investigated the optical absorption spectra, steady-state emission, excitation, and time-resolved fluorescence of Au^0 for $AuClP(C_2H_5)_3$ in MTHF, in which the production of the Au^0 has been already confirmed by ESR observation.

Experimental Section

$AuClP(C_2H_5)_3$ of stated purity of more than 97%, which is one of the typical chemical compounds of Au(I), was purchased from Tri Chemical Laboratories Inc. and was used without further purification. Reagent grade MTHF was distilled fractionally, and no optical absorption due to its chemical additives was observed in the region of wavelengths longer than 230 nm. An amount of 10 mL of MTHF was first bubbled by N_2 gas sufficiently to remove oxygen molecules in the solvents. The solute was then added. Incidentally, to compare the effect of removal of oxygen molecules in the solvents, Ar gas was also used for bubbling the solvent. However, no difference was observed in the results of emission and excitation spectra for both cases. The concentrations of Au^+ ions ($[Au^+]$) were 0.01 and 0.05 M for the measurements of optical absorption spectra, and $[Au^+] = 0.05$ and 0.08 M for the measurements of steady-state emission, excitation spectra, and time-resolved emission spectra. The procedures of sample preparation were the same as in our previous studies.[6] The fresh solutions were transferred into optical cells of 1 mm path length for optical absorption measurements and ESR tubes of 4 mm inner diameter for emission measurements. The solutions were then immersed into liquid nitrogen.

The samples were γ-irradiated at 77 K at a dose rate of 22 kGy h^{-1}. Total dose was typically 22 kGy. After γ-irradiation, the samples were illuminated with light of wavelengths longer than 540 nm from a 500 W halogen lamp through an interference filter (Toshiba O-54) in order to photobleach trapped electrons. The experimental apparatus and procedures for the optical absorption measurements at 77 K were described elsewhere.[1,2] Emission and excitation spectra were measured at 73 K with use of a Hitachi fluorescence spectrophotometer (model F-4500). Color filters, for example ,UV22, UV29, UV30, UV34, UV35, L42, Y44, Y48, were used for the removal of scattered excitation light in the measurements. We investigated the time dependence of the emission spectra over the range of 2000 ms using the mode of lifetime measurements of phosphorescence. The time-resolved emission measurements at 77 K were carried out with a pulsed nitrogen laser (LN120C by Laser Photonics) and Picosecond Fluorescence Lifetime Measurement System (C4780 by Hamamatsu Photonics). The details of the specifications of these apparatuses and the photon counting methods used in this system were essentially the same as described in our previous study for silver atom.[3] In addition to the light pulses of 337 nm from nitrogen laser, two light pulses of 380 and 420 nm from the dye laser were used. These were obtained by BPBD and carbostyril solutions pumped by N_2 laser, respectively. The measurements were carried out for various full sweep ranges from 10 ns to 200 μs when excitation wavelengths of 337 and 380 nm were used. When excitation wavelengths of 420 nm were used, however, the intensity of the emission was too weak to observe the time-resolved emission spectrum so that the measurement could be carried out only for sweep full range of 200 μs.

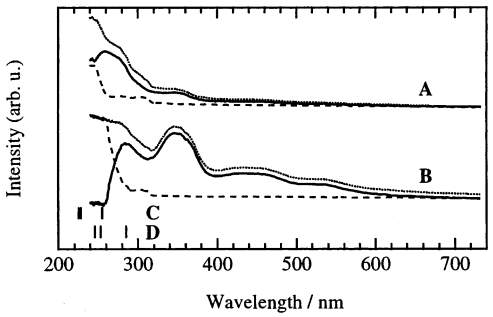

Figure 1. Absorption spectra measured at 77 K for the glassy MTHF solutions of (A) 0.01 M and (B) 0.05 M $AuClP(C_2H_5)_3$. The broken and dotted lines represent the spectra obtained before and after γ-irradiation, respectively. The solid lines represent the difference spectra. The stick diagrams are the absorption lines due to Au^0 deposited directly in solid argon (C) (ref 10) and cyclohexane (D) (ref 11) matrixes at 10−15 K.

Results and Discussion

Optical Absorption Spectra. The optical absorption spectra before γ-irradiation were subtracted from those after irradiation. The difference spectra thus obtained for MTHF solutions containing $AuClP(C_2H_5)_3$ of 0.01 and 0.05 M at 77 K are shown in Figure 1A and B, respectively. The spectra obtained before and after γ-irradiation are also shown.

For the samples of both concentrations, an absorption band was observed in the wavelength region shorter than 260 nm before γ-irradiation. After γ-irradiation, a broad, intense absorption band including at least two bands was observed in the UV region of 260−280 nm. In the difference spectrum obtained for the solution of 0.05 M, a peak appears at 280 nm, but it is not a real one because the spectrum after γ-irradiation is saturated in intensity at the wavelength. The absorption band including at least two bands must also exist in the UV region of 260−280 nm for the solution of 0.05 M. In addition to this band, a broad absorption band appeared in the NUV region of 320−380 nm after γ-irradiation. This band, which was observed easily for the solution of higher Au^+ concentration, is characteristic of the solid solutions. It seems that the broad bands in the NUV region consist of two or more components. In fact, we showed previously[1,7] that the absorption spectra of Ag^0 and Cu^0 produced in γ-irradiated solid solutions at 77 K consisted of multiple components. In Figure 1 C and D, the absorption lines due to Au^0 deposited directly in solid argon[10] and cyclohexane[11] matrixes at 10−15 K are shown by the stick diagrams, respectively. These lines are assigned to the transition from $Au^0(5d^{10}6s, 2S_{1/2})$ to $Au^{0*}(5d^{10}6p, 2P_{1/2})$ and $Au^{0*}(5d^{10}6p, 2P_{3/2})$. The absorption band of 260−280 nm observed in this study was closer to those lines in solid cyclohexane[11] matrix rather than in solid argon matrix.[10] On the basis of the ESR evidence of formation of Au^0 in our previous study,[6] together with the spectral analogy to the previous results of the optical

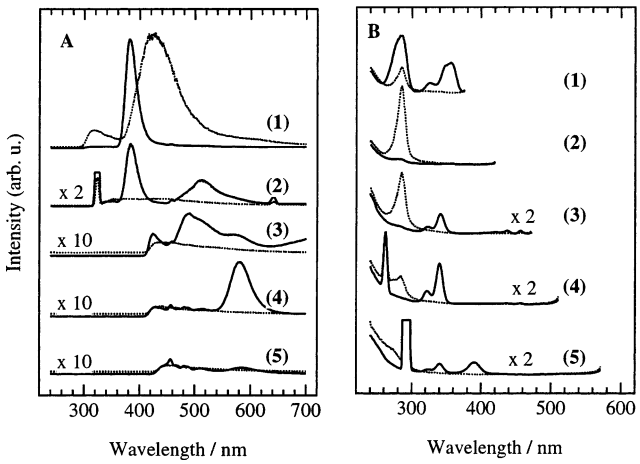

Figure 2. Steady-state emission (A) and excitation (B) spectra at 73 K of Au^0 produced in γ-irradiated MTHF solution containing 0.05 M $AuClP(C_2H_5)_3$. The dotted lines are the spectra for the samples before γ-irradiation. In the emission spectra, the wavelengths of light used for excitation are (1) 280, (2) 320, (3) 350, (4) 390, and (5) 410 nm. The excitation spectra are recorded for the peak wavelengths of emission bands at (1) 385, (2) 430, (3) 480, (4) 520, and (5) 580 nm. The ordinates represent emission intensity in arbitrary unit.

absorption of Ag^0 or Cu^0 in the solutions including Ag^+ or Cu^+ ions at 77 K,[1,7] we attribute the difference spectra to the absorption bands of Au^0 formed in the solutions at 77 K. These bands are red-shifted and broadened compared to those in rare gas matrixes, indicating a strong solvent−Au^0 interaction. For the case of higher Au^+ concentration, the weak, broad absorption bands were observed in the region of 420−480 nm and around 520 nm and will be shown later to be also attributed to Au^0 according to the results of emission measurements.

Steady-State Emission and Excitation Spectra. The steady-state emission spectra were measured at 73 K for Au^0 produced in the irradiated solid solutions of MTHF which contained Au^+ ions of various concentrations. The spectra obtained before and after γ-irradiation for $[Au^+] = 0.05$ M are shown in Figure 2A. The wavelengths for excitation light (λ_{exc}) were chosen from the wavelength region of the prominent absorption bands. The dotted and solid lines represent the emission spectra obtained before and after γ-irradiation, respectively. The respective excitation spectra corresponding to the emission bands are shown in Figure 2B.

Before γ-irradiation, an intense, broad emission band extending from 360 to 520 nm with a peak at 430 nm was observed for $\lambda_{exc} = 280$ nm which corresponds to the absorption band in UV region. This is shown by the dotted line in Figure 2A (1). This emission band disappeared after γ-irradiation, but instead a new, sharp emission band appeared at 385 nm, as shown by the solid line in Figure 2A (1). The intensity ratio of the emission band at 385 nm to that at 430 nm was about 0.4. A similar, but not identical, phenomenon was observed in the case of Cu^0 in our previous study.[7] In the case of Cu^0, the emission band at 520 nm was observed for the samples containing Cu^+ ions before γ-irradiation, but no emission was observed after γ-irradiation for $\lambda_{exc} = 250$ nm. Thus we have concluded that photoionization occurred at 250 nm in the case of Cu^0. Contrary to this, photoionization does not have a quantum yield near unity in the case of Au^0 at least for $\lambda_{exc} = 280$ nm, since the emission at 385 nm was observed for $\lambda_{exc} = 280$ nm. From the analogy with Cu^+ ions, we infer that Au^+ ions associate with ligands to form an ion−ligand complex, which is supposed to absorb light of 280 nm, and that the emission band at 430 nm is due to such complexes as $(Au^+ \cdot Ln)^*$ where L*n* represents *n* ligand molecules. The reduction in the intensity of the emission band at 430 nm after irradiation is a consequence of the conversion of Au^+ ions to Au^0. It follows that the emission band at 385 nm is due to the complexes involving Au^0. From the excitation spectra obtained before and after γ-irradiation for the monitoring wavelengths (λ_{mon}) of 385 and 430 nm, as shown by the dotted and solid lines in Figure 2B (1) and (2), respectively, it seems that the emission band at 385 nm originates from excitation at wavelengths shorter than 280 nm, whereas the emission band at 430 nm originates mainly from the absorption band at 280 nm.

In the case of $\lambda_{exc} = 320$ and 350 nm, which are wavelengths in the absorption band in the NUV region, the emission spectra after γ-irradiation show more complex profiles. They consist of at least four bands with peaks at 385, 480, 520, and 580 nm. The emission band at 520 nm was observed for $\lambda_{exc} = 320$ nm together with the emission band at 385 nm, as shown in Figure 2A (2). The emission band at 520 nm is quite broad and extends to both wavelength sides, in which the other emission bands at 480 and 580 nm are included. The absorption band in the NUV region has a peak at 350 nm as shown in Figure 1, and it seems that there is no significant absorption band at 320 nm in the NUV region. The fact that the excitation spectra showed a peak at 320 nm when monitored at 385, 480, 520, and 580 nm indicates the existence of absorption band around 320 nm. Aside from this, however, the peaks observed at 320 and 640 nm in Figure 2A (2) are due to the excitation light passed through the cutoff filter (UV34) and its second sub harmonic oscillation, respectively. For $\lambda_{exc} = 350$ nm, which is characteristic of the absorption band of the solid solutions, the emission spectra were also observed in the wavelength region of 480−600 nm. This is shown in Figure 2A (3). The emission band consists of three bands at 480, 520, and 580 nm, which were observed with the maximum intensity for $\lambda_{exc} = 350$, 320, and 390 nm, respectively. These are shown in Figure 2A (3), (2), and (4), respectively. The excitation spectra for $\lambda_{mon} = 480$, 520, and 580 nm imply that these emission bands are caused by excitation in the absorption band groups of (320 and 340 nm), (320 and 340 nm), and (320, 340, and 390 nm) as shown in Figure 2B (3), (4), and (5), respectively. The relations between the emission bands and the absorption bands observed in this study are summarized and listed in Table 1.

In addition to the emission bands mentioned above, there was a group of the very weak peaks in the wavelength region of 450−520 nm for $\lambda_{exc} = 390$ and 410 nm. This is shown in Figure 2A (4) and (5). Though the intensities of these peaks were too weak to clearly determine their structure, we confirmed that they had a characteristic structure corresponding to a mirror image of the absorption spectrum of Au^0 in the gas phase. It is noted that the intensity of these emission peaks increased and that the structure became obvious after storage in the dark at liquid nitrogen temperature. The samples were stored in liquid nitrogen for three months, and then the steady-state emission and excitation spectra were measured again at 77 K. These spectra are shown in Figure 3A and B, respectively. The emission peaks at 456, 482, 484, and 520 nm were always observed for $\lambda_{exc} = 280$, 320, 350, 390, and 410 nm. It is clear that the emission peaks at 450−520 nm are due to species produced by γ-irradiation and that the yield of species is increased during storage at 77 K. The reduction in intensity of the emission band at 385 nm is greater than that of the emission band at 520 nm during storage for three months at 77 K. Concomitantly, the peak intensity at 456 nm slightly increases. It follows that the emission bands at 385 and 520 nm are due

TABLE 1: Relations between the Emission Bands and the Absorption Bands of Au^0 Produced at 77 K in γ-Irradiated MTHF Solutions Containing 0.05 M $AuClP(C_2H_5)_3$

emission bands, nm	absorption bands which contribute to the emission bands in the left column, nm								
385	260[a]	285	320	340	360				
430		285[a]							
480			320	340[a]				440	460
456, 482,484, 520		285	320	340[a]			420	440	460
520			320	340[a]				440	460
580			320	340		385[a]			

[a] The absorption band which contributes mainly to the emission bands in the left column.

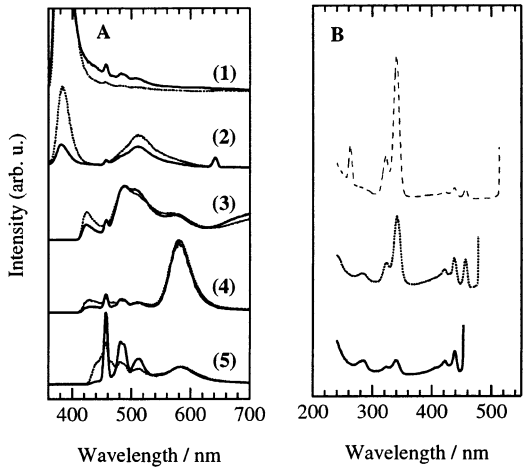

Figure 3. (A) Emission and (B) excitation spectra measured at 77 K after storage for 3 months at 77 K for the same sample after the measurements of the steady-state emission and excitation spectra shown in Figure 2. The spectra represented by dotted lines in (A) (1)−(5) are from the solid lines in Figure 2 A (1)−(5), respectively. The wavelengths of light used for excitation are (1) 280, (2) 320, (3) 350, (4) 390, and (5) 410 nm, respectively. All of the spectra were normalized to the peak intensities at (1) 385, (2) 640, (3) 485, (4) 580, and (5) 580 nm. The solid, dotted, and broken lines in (B) represent the excitation spectra monitored at 460, 485, and 520 nm, respectively.

to different species produced by irradiation. This is also evidenced by the difference in the excitation spectra monitored at 385 and 520 nm as shown in Figure 2B(1) and (4), respectively.

For $\lambda_{exc} = 350$ nm, as shown in Figure 3A (3), the emission peak at 456 nm becomes clear and the emission peak at 520 nm increases more than the emission peak at 485 nm during storage. As mentioned in the optical absorption spectra in Figure 1, the intensity of the absorption band at 350 nm depends strongly on the concentration of Au^+ ion. This reminds us of the fact that the dimer cation, $[Ag_2^+]$, is formed in the concentrated solution of Ag^+ ions.[5] However, the formation of the dimer cation, $[Au_2^+]$, was not confirmed in the previous ESR study of Au solid solution.[6]

The increase in the intensities of the emission peaks at 450−520 nm in question during storage at 77 K can be confirmed clearly in the case of $\lambda_{exc} = 390$ and 410 nm, as shown in Figure 3A (4) and (5), respectively. It is noted that the spectral profile of the emission bands in the region of 450−520 nm looks like a mirror image of the absorption spectra of Au^0 in the rare gas matrix.[10] If this is the case, the emission bands can be attributed to Au^{0*} trapped in a large cavity where Au^0 scarcely interacts with solvent molecules. Thus, the excitation spectra monitored at these emission bands must include the absorption bands corresponding to $Au^{0*}(5d^{10}6p, 2P_{1/2})$ and $Au^{0*}(5d^{10}6p, 2P_{3/2})$. Figure 3B shows the excitation spectra recorded for wavelengths of 460, 485, and 520 nm near by the peaks of the emission bands in question, i.e., 456, 482, 484, and 520 nm. It follows from the spectra that the absorption bands at 260, 280, 320, 340, 420, 440, and 460 nm are responsible for the characteristic emission bands at 450−520 nm. The peak at 260 nm observed in the excitation spectrum for $\lambda_{mon} = 520$ nm is mainly second harmonic oscillation of the monitoring light, so it is not clear to what extent the band at 260 nm contributes. However, it is true that there is an absorption band due to Au^0 at 260 nm and that this band is responsible for the emission at 520 nm. Considering the assignments in the rare gas matrixes,[9,10] we infer that the absorption bands at 260−280 nm are attributed to the doublet of $Au^{0*}(5d^{10}6p, 2P_{3/2})$ and that the absorption band at 320 or 340 nm is attributed to $Au^{0*}(5d^{10}6p, 2P_{1/2})$. The excited gold atoms in $2P_{1/2}$ and $2P_{3/2}$ states participate mainly in the formation of the emissive exciplexes which are proposed later. The 2-fold splitting of $(5d^{10}6p, 2P_{1/2})$ may be due to a field effect of matrix or different trapping sites of Au^0.

We have no knowledge of a transition of Au^0 corresponding to the absorption bands at 420, 440, and 460 nm that were observed for $\lambda_{mon} = 460$, 480, and 520 nm. At the present stage, we infer that those are attributed to the transition involving 5d−6s. This is a forbidden transition, but it may happen when configuration mixing such as spin−orbit coupling occurs. As Baetzold[13] has pointed out, the interaction between *s* and *d* valence orbitals is greater in gold than in silver because these atomic energy levels are closer in gold than in silver. Thus 5d−6s transition possibly occurs when Au^+ ions remain in the samples after γ-irradiation. The hypothesis of configuration mixing of *d* valence orbitals accommodates the results of ESR measurement in the previous study:[6] The *g* shift, $g_J - g_{J,free}$, is negative for Ag^0,[16] which is expected to occur by an admixture of the wave function of the atom in its $2S_{1/2}$ state into the *p* orbital. On the contrary, the observed positive shift for Au^0 [23] and Cu^0 [7] is explained by the hypothesis that the free atom configurations of Au, $5d^{10}6s^1$, and $3d^{10}4s^1$ for Cu admixes into $d_{x^2-y^2}$ to some extent rather than *p* orbital for the systems studied. An alternative explanation can be based on the molecular orbital energy level for $Au(O_2)$ as proposed by McIntosh et al.[12] When the Au^0 in its excited state produced by γ-irradiation in the MTHF matrix is coupled with ligand solvent molecules to form the exciplex, the oxygen atom of the MTHF molecule will reorient to the Au^0 side. If two MTHF molecules participate in the configuration, the energy levels of the exciplex will be close to those of $Au(O_2)$.

Time-Resolved Emission Spectra. The two kinds of measurements were carried out to investigate the time dependence of the emission intensities: One is the phosphorescence with lifetimes longer than milliseconds and the other is the fluorescence with lifetimes shorter than that.

In the case of $\lambda_{exc} = 280$ nm, the time-dependent spectra of phosphorescence were observed for $\lambda_{mon} = 430$ nm before γ-irradiation and $\lambda_{mon} = 385$ nm after γ-irradiation, and are shown in Figure 4A and B, respectively. The lifetime of the

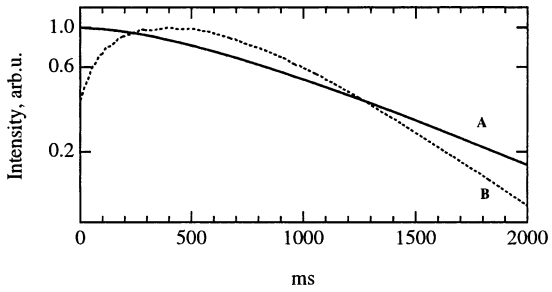

Figure 4. Typical decay profiles of phosphorescence measured at 73 K for the samples stored at 77 K for three months after the measurements of the steady-state emission and excitation spectra and time-resolved fluorescence spectra. The decay profiles were obtained by (A) $\lambda_{exc}/\lambda_{mon}$ = 280 nm/430 nm before γ-irradiation and (B) $\lambda_{exc}/\lambda_{mon}$ = 280 nm/385 nm after γ-irradiation, respectively, where λ_{exc} and λ_{mon} represent the wavelength of the excitation light and that of the monitoring light, respectively. The lifetimes obtained by assuming single-exponential decay for (A) and the cascade decay for (B) are 625 ms for (A), and 146 ms and 461 ms for (B), respectively.

phosphorescence at 430 nm observed before γ-irradiation was about 625 ms.

The emission band at 430 nm is assigned to the phosphorescence from $(Au^+ \cdot Ln)^*$. The spectral profile of the phosphorescence for λ_{exc} = 280 nm was similar to that of the steady-state emission spectrum for λ_{exc} = 280 nm. The component of the phosphorescence in the emission band at 385 nm is estimated to be roughly 44% of the total intensity of the emission band at 385 nm. No other phosphorescence was observed around the emission bands at 480, 520, and 580 nm after γ-irradiation. Considering this result, together with the fact that the absorption bands at around 260−280 nm are close to the doublet transitions ($2P_{3/2} \leftarrow 2S_{1/2}$) for Au^0 in the solid rare gases,[9,10] we infer that the emission band at 385 nm is due to a complex consisting of both Au^+ and Au^0. Since the dimer cation of Au^0 has not been observed in our previous ESR study,[6] the most plausible state for the 385 nm emission is $(Au^0 \cdot Ln)^*...Au^+$, where exciplex $(Au^0 \cdot Ln)^*$ interacts weakly with a nearby Au^+ ion.

It is noted that the decay profile of the phosphorescence at 385 nm does not show a simple decay pattern, but includes a formation pattern. Assuming the cascade reaction as follows:

$$(Au^0 \cdot Ln...Au^+)^* \xrightarrow{k_1} (Au^0)^*...(Ln \cdot Au^+)^* \xrightarrow{k_2} (Au^0)...(Ln \cdot Au^+) \quad (1)$$

or

$$(Au^0) \cdot Ln...Au^{+*} \xrightarrow{k_1} (Au^+ \cdot Ln...Au^0)^* \xrightarrow{k_2} (Au^+ \cdot Ln)...(Au^0) \quad (2)$$

the fitting analysis for the time-dependence spectra of the phosphorescence was carried out. The rate constants obtained were $k_1 = 4.7\ s^{-1}$ and $k_2 = 1.5\ s^{-1}$. It follows that the triplet states of the species of $(Au^0)^*...(Ln \cdot Au^+)^*$ or $(Au^+ \cdot Ln...Au^0)^*$, is formed with lifetime of 146 ms and simultaneously decays to the ground singlet state with lifetime of 461 ms.

The two-dimensional time-resolved emission spectra of Au^0 produced in γ-irradiated MTHF solid solutions of $[Au^+]$ = 0.05 and 0.08 M were investigated for λ_{exc} = 337, 380, and 420 nm. Typical streak images obtained for λ_{exc} = 337 nm in the full sweep range of 200 μs are shown in Figure 5 A and B.

The wavelength profile for $\lambda = 520 \pm 68$ nm, as shown in Figure 5B, was almost the same as obtained for the steady-state measurement. This means that the emission processes included in this image frame finish within 200 μs. The intensity of the emission bands at 385 nm in Figure 5A is considerably weaker than that obtained for the steady-state measurement in comparison with the intensity of the broad emission band at 520 nm. This is due to the fact that the contribution of phosphorescence in the emission band at 385 nm can be observed in the steady-state emission measurement, but not in the time-resolved measurement in the full sweep range of 200 μs. In the streak image for $\lambda = 370 \pm 68$ nm, as shown in Figure 5A, the excitation light at 337 nm and the emission band at 385 nm were observed in the same frame. It can be seen that the latter delayed about 1−5 μs after the former. However, we could not observe the rise time of the emission band at 385 nm precisely on this time scale because of the difficulty of obtaining good accuracy in the measurements for the full sweep range of 1 or 5 μs, similar to the case of Ag^0.[3] By analogy with the Ag^0 case, Au^0 coupled with matrix molecules in its excited state forms such exciplex as $(Au^0 \cdot Ln)^*...Au^+$, followed by a simultaneous relaxation to an emissive state after 1−5 μs, giving rise to the emission except for the phosphorescence in the emission band of 385 nm. The intensity of the emission in the wavelength region of 500 ± 68 nm for λ_{exc} = 380 nm is too weak to determine the lifetime precisely, as shown in Figure 5C. Nevertheless, a weak emission band can be seen in the wavelength region of 450−520 nm. By time-resolved measurement with the full sweep range of 100 ns, it was confirmed that the lifetime of this group of emission peaks was shorter than 50 ns. The emission band in wavelength region of d in Figure 5D is the same as the emission band of 580 nm observed for λ_{exc} = 390 nm in the steady-state emission spectra in Figure 2B (4). The intensity ratio of the emission band at 580 nm to the group of emission peaks at 450−520 nm obtained for the time-resolved emission measurement does not contradict the results of the steady-state emission measurement.

The typical time profiles for the full sweep range of 200 μs for 385 ± 10 nm, 480 ± 10 nm and 520 ± 10 nm obtained at λ_{exc} = 337 nm and that of 580 ± 20 nm obtained at λ_{exc} = 380 nm are shown in Figure 6. It is shown in Figure 6 that there are several components with different lifetimes. The lifetimes obtained are listed in Table 2.

The results of lifetime analysis fall into three groups; τ_{short} (0.7−0.9 μs), τ_{middle}(5.0−6.3 μs) , and τ_{long}(10.2−24.7 μs). The main component with τ_{middle} of the emission bands of a(385 nm) and b(480 nm) is attributed to the exciplex as $(Au^0 \cdot Ln...Au^+)^*$ like the dimer cation $(Ag^0 \cdot Ag^+)^*$ in the case of Ag^0. In the same way, the main component with τ_{long} of the emission bands of c(520 nm) and d(580 nm) is attributed to the exciplex as $(Au^0 \cdot Ln)^*$ by analogy with $(Ag^0 \cdot Ln)^*$ for Ag^0.

Considering the present results together with the previous ESR results, the emissive excited species can be classified roughly into four types and their formation mechanisms are schematically illustrated in Figure 7.

The first type is $(Au^+ \cdot Ln)^*$, that gives rise to the absorption band at 280 nm, in which an excited Au^+ ion associates with ligand molecules to form an ion−ligand complex, being followed by the intense, broad phosphorescence at 430 nm with a lifetime of about 625 ms.

The second type is $(Au^0 \cdot Ln...Au^+)^*$ that gives rise to the absorption bands at around 270 nm and the intense emission band at 385 nm. This emission band is almost analogous to the main component of the emission band (E_1) of Ag^0, which was attributed to the dimer cation, $(Ag^0 \cdot Ag^+)^*$. However, we could not find evidence for the formation of the dimer cation in the case of Au^0 and confirmed that about 44% of the intensity of

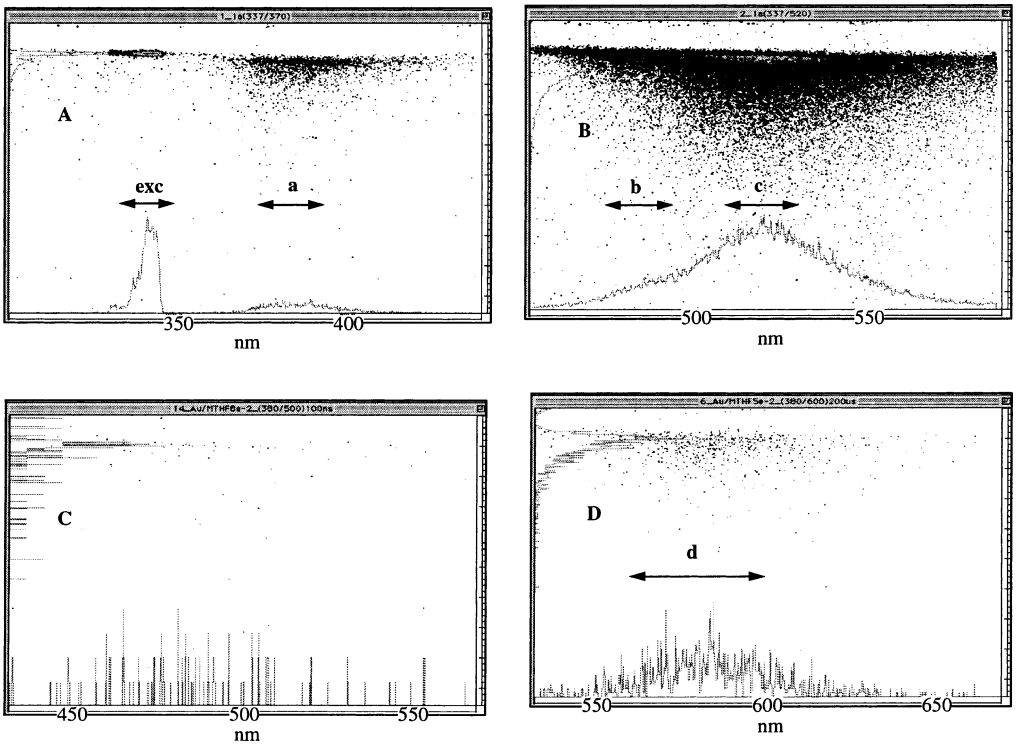

Figure 5. The typical streak pictures and spectra measured at 73 K after γ-irradiation at 77 K in the wavelength ranges of (A) 370 ± 68 nm and (B) 520 ± 68 nm obtained by N_2 laser excitation at 337 nm, (C) 500 ± 68 nm and (D) 600 ± 68 nm obtained by dye laser excitation at 380 nm. The horizontal and vertical axes are wavelength and time scales with 630 and 480 channels, respectively. The full sweep range of time axis was 200 μs for A, B, and D. The full sweep range of time axis was 100 ns for C.

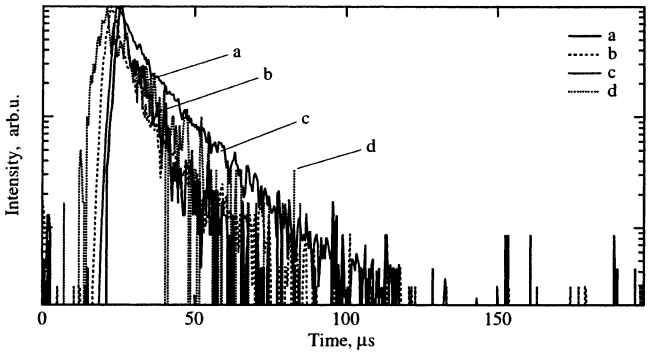

Figure 6. The time profiles for the emissions of (a) 385 ± 10, (b) 480 ± 10, (c) 520 ± 10, and (d) 580 ± 20 nm in the wavelength region represented by the arrows in the streak images of Figure 5A, B, and D.

TABLE 2: Lifetimes Calculated from the Time Profiles in the Full Sweep Range of 200 μs by Assuming That Every Decay Curve Consists of Two Components

emission bands	τ_1 [μs]	τ_2 [μs]	I(τ_1) %[a]
a(385 nm)	0.7	6.3	33.4
b(480 nm)	5.7	24.7	70.5
c(520 nm)	5.0	15.3	32.9
d(580 nm)	10.2	0.9	76.7

[a] The ratio of the intensity of τ_1 component to that of total band in percent.

the emission at 385 nm was due to phosphorescence. The species (Au^+·L*n*...Au^0)* formed by reaction 2 emits phosphorescence with a lifetime of 461 ms. The emission band at 385 nm, except for this phosphorescence, consists of two components with different lifetimes; the main component with $\tau = 6.3$ μs, which is about 37.5% in intensity of all the emission band at 385 nm, is assignable to (Au^0·L*n*...Au^+)*. This exciplex is formed by coupling strongly with solvent molecules and interacts weakly with a nearby Au^+ ion. The emission originates from an equilibrium state, which is populated from an unrelaxed Franck−Condon state. The component with $\tau = 0.7$ μs, which is about 18.5% in intensity of the entire emission band at 385 nm, may be due to exciplex (Au^0)*...L*n*.

The third type is (Au^0·L*n*)* that gives rise to VIS absorption bands, in which Au^0 in its excited state in MTHF solid solution is strongly coupled with matrix molecules to compose the exciplex. This exciplex shows fluorescence bands at 480, 520, and 580 nm with lifetimes of 10.2−24.7 μs.

The fourth type is (Au^0)* that is trapped in a large cavity in which Au^0 in its excited state interacts very weakly with the surrounding solvent molecules. The fluorescence spectrum with peaks at 456, 482, 484, and 520 nm shows the mirror image of the absorption spectrum of gold atoms observed in rare gas matrixes. It is also confirmed that the formation of this emissive (Au^0)* develops upon storing the irradiated sample at 77 K. This is explained by assuming the reaction of electron transfer from ligand solvent molecules to Au^+ such as (Au^0·L*n*...Au^+)* → 2(Au^0)*. This hypothesis accommodates the fact that the intensity of the emission band of 385 nm attributed to (Au^0·L*n*...Au^+)* is decreased during the storage at 77 K. Although the Stokes shift indicates a strong interaction between Au^0 and solvent molecules, the amount of the shift is rather smaller than those of Ag^0 and Cu^0. This implies that the cavity of trapped (Au^0)* is larger than those for Ag^0 and Cu^0.

Conclusion

Au^0 was produced at 77 K by γ-irradiation of MTHF solutions containing Au^+. The absorption bands at around 270−280 and 340 nm were ascribed to Au^0 in the solid solutions. The weak absorption band at around 420 nm was also attributed to Au^0. These bands were red-shifted and broadened compared to those in the rare gas matrixes, indicating a strong solvent−Au^0

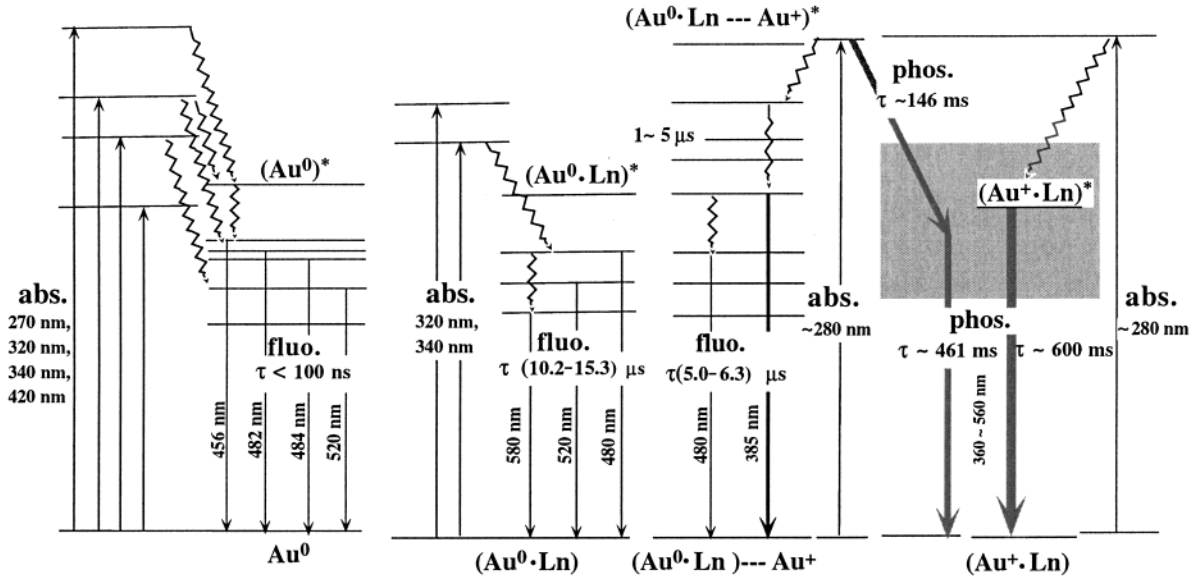

Figure 7. Schematic representation of the absorption (abs.) and emission (fluo. and phos.) mechanism of the proposed species corresponding to the emission bands observed in the present study.

interaction. Excitation of the absorption bands at around 280 nm led to phosphorescence of three kinds of lifetimes. One of them with a lifetime of about 625 ms was attributed to an exciplex such as $(Au^{+}\cdot Ln)^{*}$. As for the other two components, with lifetimes of about 146 and 461 ms, it became clear from the behavior of the time dependence profile of the phosphorescence intensity that the latter grew as the former decayed. These were ascribed to exciplexes such as $(Au^{0}\cdot Ln...Au^{+})^{*}$ and $(Au^{+}\cdot Ln...Au^{0})^{*}$, respectively. The absorption band, which was ascribed to photoionization of Au^{0}, must be around at 280 nm. The fluorescence band observed at 385 nm and a set of bands at 480, 520, and 580 nm bear close resemblance to the E_1 and E_2 bands of Ag^{0},[3] respectively. The former was attributed to the exciplex $(Au^{0}\cdot Ln...Au^{+})^{*}$ that was not a paramagnetic species. The latter was attributed to the exciplex $(Au^{0}\cdot Ln)^{*}$. The group of emission bands with peaks at 456, 482, 484, and 520 nm showed the characteristic structure of a mirror image of the absorption bands of Au^{0} in the gas phase[8] and the solid rare gas phase.[9−15] This structural profile was observed for the first time in the present study for Au^{0} produced in γ-irradiated organic solid solutions at 77 K. These were attributed to Au^{0} trapped in a large cavity where Au^{0} in its excited state interacts very weakly with the surrounding solvent molecules.

Acknowledgment. This work has been carried out under the Visiting Researcher's Program of Research Reactor Institute, Kyoto University, on FY 2002, and also has been carried out by Grants-in-Aid for Scientific Research of Ministry of Education, Culture, Sports, Scientific and Technology, on FY 2001-2002. The authors express their sincere thanks to Dr. H. Hase who was Ex-professor of Kyoto University for his fruitful suggestions.

References and Notes

(1) Hase, H.; Arai, S.; Isomura, A.; Terazawa, N.; Miyatake, Y.; Hoshino, M. *J. Phys. Chem.* **1996**, *100*, 11534.

(2) Hase, H.; Miyatake, Y.; Hoshino, M.; Taguchi, M.; Arai, S. *Radiat. Phys. Chem.* **1997**, *49*, 59.

(3) Miyatake, Y.; Hase, H.; Matsuura, K.; Taguchi, M.; Hoshino, M.; Arai, S. *J. Phys. Chem. B* **1998**, *102*, 8389.

(4) Matsuura, K.; Liu, M.; Hoshino, M.; Hase, H.; Arai, S.; Miyatake, Y. *Chem. Phys. Lett.* **1999**, *301*, 401.

(5) Matsuura, M.; Hase, H.; Arai, S.; Miyatake, Y.; Hoshino, M. *Bull. Chem. Soc. Jpn.* **1999**, *72*, 363.

(6) Hase, H.; Miyatake, Y.; Miyamoto, Y. *Chem. Phys. Lett.* **2000**, *326*, 299.

(7) Miyatake, Y.; Hase, H.; Saito, T.; Onishi, M.; Tajima, Y.; Hoshino, M. *J. Phys. Chem. A* **2001**, *105*, 5823.

(8) Moore, C. E. *Atomic Energy Levels*; U. S. Government Printing Office; National Bureau of Standard: Washington, DC, 1949; Vol. III.

(9) Brewer, L.; King, B. *J. Chem. Phys.* **1970**, *53*, 3981.

(10) Gruen, D. M.; Gaudioso, S. L.; McBeth, R. L.; Lerner, J. L *J. Chem. Phys.* **1974**, *60*, 89.

(11) Klotzbücher, W. E.; Ozin, G. A. *Inorg. Chem.* **1980**, *19*, 3767.

(12) McIntosh, D.; Ozin, G. A. *Inorg. Chem.* **1976**, *15*, 2869.

(13) Baetzold, R. C. *J. Chem. Phys.* **1971**, *55*, 4355.

(14) Forstmann, F.; Kolb, D. M.; Leutloff, D.; Schulze, W. *J. Chem. Phys.* **1977**, *66*, 2806.

(15) Kolb, D. M.; Leutloff, D. *Chem. Phys. Lett.* **1978**, *55*, 264.

(16) Bosi, L.; Tavecchio, A.; Zelada, M. *Solid State Commun.* **1998**, *108*, 903.

(17) Ipe, B. I.; Thomas, G.; Barazzouk, S.; Hotchandani, S.; Kamat, P. V. *J. Phys. Chem. B* **2002**, *106*, 18.